01 Jan 2010

Condition Assessment of Bill Emerson Memorial Cable-Stayed Bridge under Postulated Design Earthquake

Dongming Yan

Wenjian Wang

Genda Chen
Missouri University of Science and Technology, gchen@mst.edu

Bryan A. Hartnagel

Recommended Citation

D. Yan et al., "Condition Assessment of Bill Emerson Memorial Cable-Stayed Bridge under Postulated Design Earthquake," *Transportation Research Record*, no. 2172, pp. 159-167, National Research Council (U.S.), Jan 2010.
The definitive version is available at https://doi.org/10.3141/2172-18

Condition Assessment of Bill Emerson Memorial Cable-Stayed Bridge Under Postulated Design Earthquake

Dongming Yan, Wenjian Wang, Genda Chen, and Bryan A. Hartnagel

In this study, a three-dimensional finite element model of the Bill Emerson Memorial cable-stayed bridge was developed and validated with the acceleration data recorded during the M4.1 earthquake of May 1, 2005, in Manila, Arkansas. The model took into account the geometric nonlinear properties associated with cable sagging and soil–foundation–structure interaction. The validated model was used to evaluate the performance of a seismic protective system, the behavior of cable-stayed spans, and the accuracy of two simplified bridge models that have been extensively used by the structural control community. The calculated natural frequencies and mode shapes correlated well with the measured data. Except that the hollow columns of two H-shaped towers were near yielding immediately above their capbeams, the cable-stayed spans behaved elastically as expected under the design earthquake that was scaled up from the recorded rock motions at the bridge site. The minimum factor of safety of all cables is 2.78, which is slightly greater than the design target.

Because of their aesthetic appearance, cable-stayed bridges have been widely used as river-crossing links in highway networks. With the rapid progression of analysis tools and construction technologies in recent years, the main spans of cable-stayed bridges have been pushed to the limit. Opened to traffic on June 30, 2008, the longest cable-stayed bridge, Sutong Bridge over the Yangtze River in China, is 1,088 m long. With ever-increasing span lengths, cable-stayed bridges behave in a more complex manner, often becoming more susceptible to environmental effects. The seismic performance and safety of cable-stayed bridges is of paramount interest to the affected community in the event of an earthquake.

Although subjected to significant stresses under gravity loads, cable-stayed bridges are mostly susceptible to dynamic loadings resulting from earthquakes, winds, and moving vehicles. They must be assessed to ensure smooth operation during their life span and structural safety under earthquake loads. One way to assess a structure is to conduct extensive dynamic analyses and compare load and displacement with strength and ductility to understand the behavior of the structure (*1, 2*).

Because of their complexity, long-span cable-stayed bridges are usually analyzed and evaluated with a finite element model (FEM) for their dynamic characteristics and response (*3*). Using an established FEM, Ren (*4*) and Ren and Obata (*5*) investigated the elastic–plastic seismic behavior, nonlinear static behavior, and ultimate behavior of a long-span cable-stayed bridge over the Ming River in China. Significant analyses of cable-stayed bridges were also conducted by Nazmy and Abdel-Ghaffar and by Abdel-Ghaffar and Nazmy in the past 20 years under static and earthquake loads (*6, 7*).

CABLE-STAYED BRIDGE AND SEISMIC INSTRUMENTATION

Structure and Site Characteristics

The Bill Emerson Memorial Bridge is a cable-stayed bridge spanning the Mississippi River and connecting MO-34 and IL-146 at Cape Girardeau, Missouri. The final design of the bridge includes 2 towers, 128 cables, and 12 additional piers in the approach span on the Illinois side. The bridge has a total length of 1,206 m, consisting of one 350.6-m long main span, two 142.7-m long side spans, and one 570-m long approach span on the Illinois side. The 12 piers on the approach span have 11 equal spacings of 51.8 m each. Carrying two-way traffic, the bridge has four 3.66-m wide vehicular lanes plus two narrower shoulders. The total width of the bridge deck is 29.3 m. The deck is composed of two longitudinal built-up steel girders, a longitudinal center strut, transverse floor beams, and precast concrete slabs. A concrete barrier is located in the center of the bridge, and two railings and additional concrete barriers are located along the edges of the deck. Pier 2 rests on rock and Piers 3 and 4 are supported on two separate caissons.

At each bridge tower, eight longitudinal earthquake shock transfer devices were installed between the capbeam of the tower and its connecting edge girders, and two lateral earthquake restrainers were installed between the capbeam of the tower and its connecting floorbeam between two edge girders. Each edge girder was rested on a pot bearing that is supported on top of the capbeam and is restrained by the capbeam for any transverse and lateral motions. For two towers, a total of 16 devices, 4 restrainers, and 4 pot bearings were designed for the bridge. One additional lateral earthquake restrainer and two tie-down devices were installed at each end of the cable-stayed span at Pier 1 or Pier 4, amounting to a total of six lateral earthquake restrainers on the bridge. A total of four bearings at both ends of the

D. Yan and G. Chen, Department of Civil, Architectural, and Environmental Engineering, Missouri University of Science and Technology, 1401 North Pine Street, Rolla, MO, 65409; School of Hydraulic and Environmental Engineering, Zhengzhou University, Kexue Road 100, Zhengzhou, He'nan 450001, China. W. Wang, Weidlinger Associates, Inc., 201 Broadway #4, Cambridge, MA 02139. B. A. Hartnagel, Missouri Department of Transportation, 105 West Capitol Avenue, Jefferson City, MO 65102. Corresponding author: G. Chen, gchen@mst.edu.

Transportation Research Record: Journal of the Transportation Research Board, No. 2172, Transportation Research Board of the National Academies, Washington, D.C., 2010, pp. 159–167.
DOI: 10.3141/2172-18

bridge, Bent 1 and Pier 4, were designed to allow for longitudinal displacement and rotation about the transverse and vertical axes.

The bridge is located approximately 80 km from New Madrid, Missouri, where three of the largest earthquakes in the United States have occurred. Each of the three most significant earthquakes had a magnitude of above 8.0 (*8*). During the winter of 1811 to 1812 alone, this seismic region was shaken by a total of more than 2,000 events, over 200 of which were evaluated to have been moderate to large earthquakes. In the past few years, two earthquakes with magnitudes of over 4.0 were recorded in the New Madrid Seismic Zone (NMSZ). Therefore, this bridge is expected to experience one or more significant earthquakes during its life span of 100 years. The cable-stayed bridge structure was proportioned to withstand an earthquake of M7.5 or stronger. The 30% seismic load combination rules for earthquake component effects were used in accordance with the AASHTO Division I-A specifications (*9*). These loads were then combined with the dead load applied to the bridge.

Seismic Instrumentation System

The bridge is located in a geologically changing area. Because of its critical proximity to the NMSZ, as well as lack of strong ground motion records, the bridge has been continuously monitored with a seismic instrumentation system, which consists of 84 Kinemetrics EpiSensor accelerometers, Q330 digitizers, and Baler units for data concentrator and mass storage (*10*).

Antennas were installed on two bridge towers at Piers 2 and 3, at two free-field sites on the Illinois end, and on the central recording building near the bridge on the Missouri side. Wireless communications can be initiated among various locations with antennas. The recorded data have been wirelessly transferred from the bridge and free-field sites to the off-structure central recording building on the Missouri side. The accelerometers installed throughout the bridge structure and adjacent free-field sites allow the recording of structural vibrations of the bridge and free-field motions at the surface and down-hole locations. They were deployed such that the acquired data can be used to understand the overall response and behavior of the cable-stayed bridge, including translational, torsional, rocking, and translational soil–structure interactions at foundation levels.

The monitoring system has been in operation since December 2004, and it continuously records site and structural responses from vehicular traffic and minor earthquakes. However, only the most recent 16 days of recorded data are kept on file unless a sizable earthquake has been identified. At 12:37′32″ (Universal Time) on May 1, 2005, an earthquake of M4.1 on the Richter scale occurred at 4 mi SSE (162 degrees) from Manila, Arkansas, 180 km from the bridge. The hypocenter depth was estimated to be about 10 km.

Motivation and Objectives of This Study

The Bill Emerson Memorial cable-stayed bridge was among the first of its kind to be constructed with a comprehensive seismic protective system that consists of 16 longitudinal shock transfer devices and 6 lateral earthquake restrainers. In addition, the bridge superstructure is connected to the bridge substructure by four tie-down devices and four pot bearings. The behavior and performance of the bridge greatly depend on how effective such a complicated mechanical system will be during an earthquake. As significant field-recorded data become available, it is highly desirable to verify various assumptions made in the design process and to understand the characteristics of the special structure under realistic earthquake conditions. In addition, two simplified FEMs of the bridge structure have been used extensively within the structural control research community for a series of ASCE structural control benchmark studies (*11*). How representative these models are of real-world structures will potentially affect the use of examined control technologies in practical applications.

Therefore, the objectives of this study are to develop and validate a realistic FEM of the cable-stayed bridge by using recorded ground motions in order to quantify the accuracy of the two simplified FEMs used as ASCE benchmark studies, characterize the bridge structure and study the behavior and performance of the seismic system, and assess the bridge structure and validate the design assumptions for critical components such as cables and towers.

MODELING OF CABLE-STAYED BRIDGE

The cable-stayed bridge is a complex structure, including a variety of structural and mechanical components such as towers, cables, decks, girders, beams, shock transmission devices, lateral earthquake restrainers, and bearings. To represent the main components of the bridge structure and to reduce the degrees of freedom in the analysis model, plate elements were used to model bridge decks, frame and cable elements were to used model stay cables, and frame elements were used to model towers, girders, and beams. Constraining joints were introduced to simulate the conditions of shock transmission devices, lateral earthquake restrainers, tie-down devices, and bearings.

Because of high axial forces and bending moments, both bridge towers were modeled in detail, including the effect of steel reinforcement on their section properties. In the FEM, nonprismatic members, such as pier capbeams or towers, were represented by elements of varying section properties. The elevation difference of various structural members to accommodate the transverse grade and the longitudinal profile of the bridge roadway was also taken into account. An infill wall enclosed by the bottom portions of two vertical columns and the capbeam of each wall was included in the FEM.

The modeling of cables requires close attention to their sagging-induced geometric nonlinearity and their end connections. As shown in Figure 1, two rigid links were introduced to connect each cable to the neutral axis of the girder and the tower, respectively. The use of rigid links ensures that the theoretical lengths, horizontal angles, and the maximum sag of the cables are exactly the same as designed.

The modeling of restraint conditions at devices, bearings, and expansion joints requires careful considerations to their continuity of displacement components in horizontal, longitudinal, and vertical directions. Each lateral earthquake restrainer located at the midspan of the capbeam at Piers 1 to 4 was modeled to provide lateral restraints between the floorbeam and the capbeam. Each pair of earthquake shock transmission devices was modeled as one longitudinal roller.

Since Pier 2 is based on rock and Piers 3 and 4 are supported on massive caissons, soil–pile interaction effects can be neglected in the cable-stayed span. In contrast, Piers 5 to 14 in the Illinois approach are supported on pedestal pile-group foundations. In the FEM, the soil–pile interaction was simulated by linear dashpots and springs in longitudinal, transverse, and vertical directions. The entire bridge structure was modeled as shown in Figure 1 based on the geometries and material data from as-built drawings. The FEM of the entire

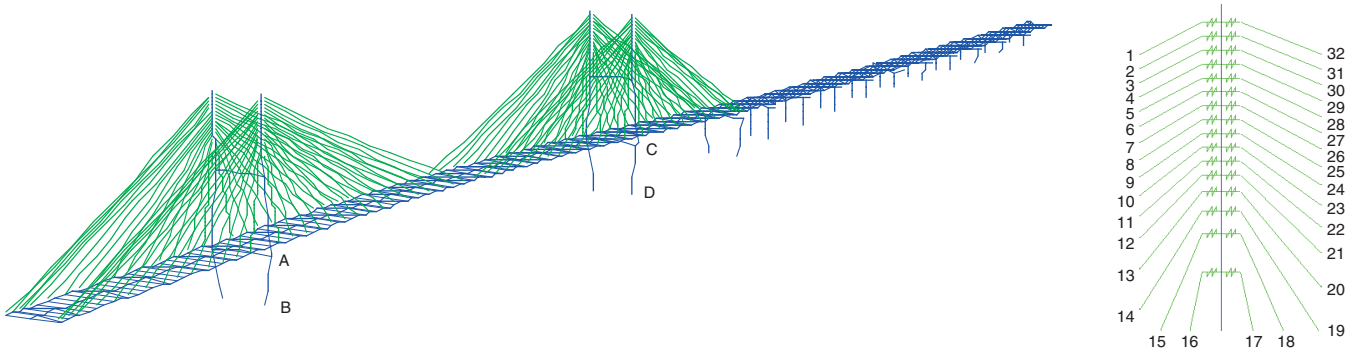

FIGURE 1 Full three-dimensional FEM of bridge.

bridge has a total of 3,075 joints, 3,622 frame elements, 106 shell elements, and 853 two-dimensional solid elements, resulting in a total of 15,926 degrees of freedom.

FEM VALIDATION

Validation by Natural Frequency

The calculated frequencies from the FEM of the bridge are compared in Table 1 with the identified frequencies from the measured acceleration records for 16 modes of vibration up to 17.94 Hz. It can be seen from Table 1 that most of the calculated frequencies match their corresponding measured frequencies very well with a maximum error of less than 10% of their respective measured frequencies. For the modes of vibration included in Figure 2, the computed frequencies are plotted in Figure 3 against the measured frequencies. Considering a 45-degree regression line, the coefficient of regression of the calculated and measured frequencies was determined to be $R^2 = .996$. This coefficient indicates a good correlation between the calculated and the measured frequencies. It is noted that the fourth, fifth, and ninth modes of the bridge are not included in Table 1 because their mass participations are negligible.

The natural frequencies determined from the two simplified models [C-shape model and spine model from Caicedo et al. (*12*)] are also included in Table 1. In comparison with the C-shape model, the fundamental frequency of the FEM is 7% higher, indicating that the C-shape model underestimated the stiffness of the bridge structure likely because of the neglect of diaphragm actions of the bridge deck. In comparison with results by Caicedo et al. (*12*), Figure 2 indicates that the shapes of the first three dominant modes with significant mass participations seem comparable between the FEM and the C-shape model. As pointed out by Caicedo et al. (*12*), the spine model was even less accurate. Indeed, the natural frequencies determined by the C-shape model are all closer to those of the FEM in this study.

Validation by Mode Shape

The FEM was further validated by comparing the graphical representations of corresponding calculated and identified shapes of the first three modes of vibration as shown in Figure 4. To evaluate the

TABLE 1 Comparison of Calculated and Measured Natural Frequencies

No.	Mode	FEM (Hz)	Measured (Hz)	Error (%)	Spine Model (Hz)	C-Shape Model (Hz)
1	1	0.32	0.34	–4.14	0.2978	0.3034
2	2	0.39	0.42	–7.76	0.3978	0.3981
3	3	0.47	0.50	–5.51	0.5264	0.4711
4	6	0.60	0.59	2.59	0.6575	0.6717
5	7	0.65	0.65	0.01	0.6772	0.6791
6	8	0.70	0.71	–2.37	0.7363	0.7029
7	10	0.75	0.78	–2.67	0.8801	0.7379
8	11	0.79	0.83	–4.13		
9	14	0.90	0.85	5.97		
10	32	1.08	1.07	0.04		
11	265	2.13	2.34	–9.94		
12	372	3.46	3.26	5.57		
13	454	9.27	8.78	5.39		
14	466	12.18	12.01	1.36		
15	474	16.02	16.15	0.06		
16	477	17.94	18.03	–0.38		

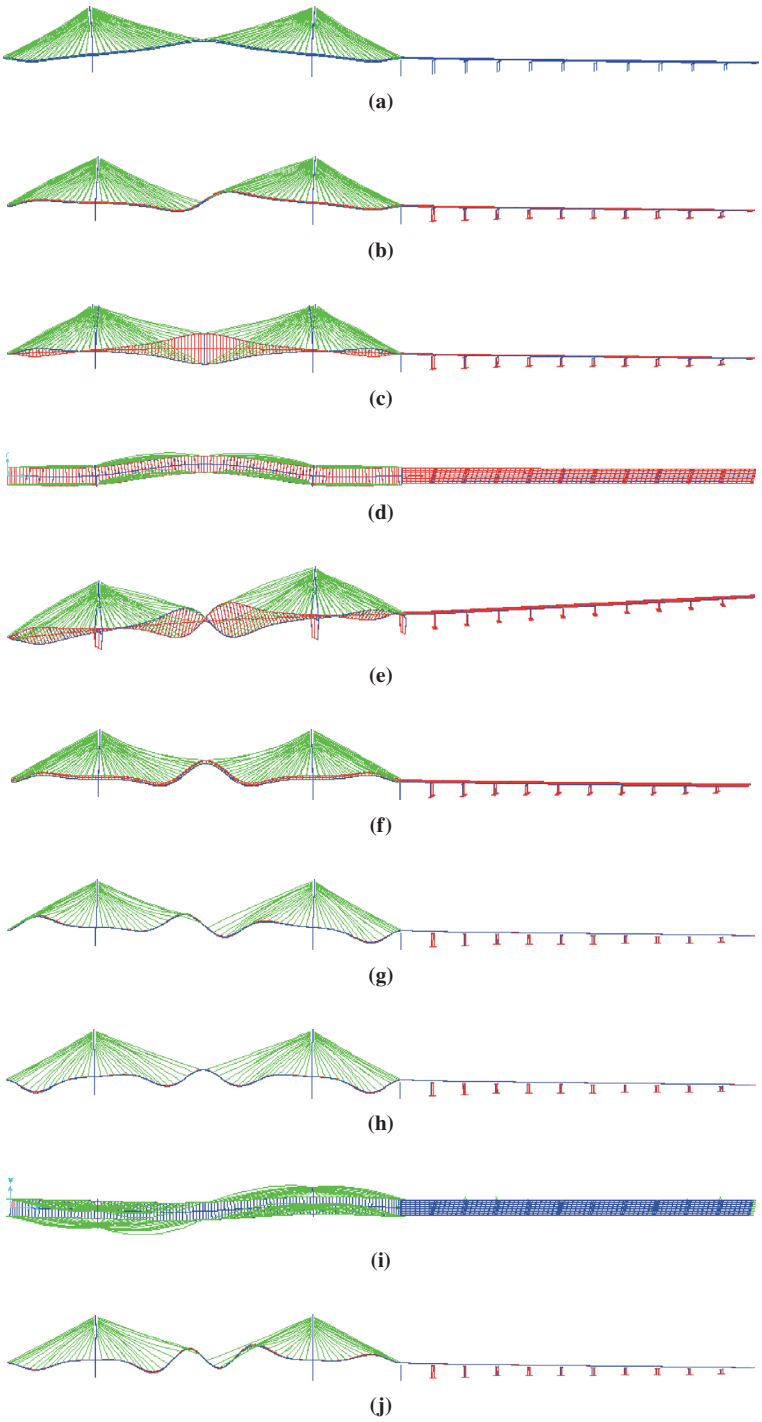

FIGURE 2 First 10 natural modes of bridge: (*a*) first mode shape (0.32 Hz), (*b*) second mode shape (0.39 Hz), (*c*) third mode shape (0.47 Hz), (*d*) fourth mode shape (0.53 Hz), (*e*) fifth mode shape (0.57 Hz), (*f*) sixth mode shape (0.60 Hz), (*g*) seventh mode shape (0.65 Hz), (*h*) eighth mode shape (0.70 Hz), (*i*) ninth mode shape (0.70 Hz), and (*j*) 10th mode shape (0.75 Hz).

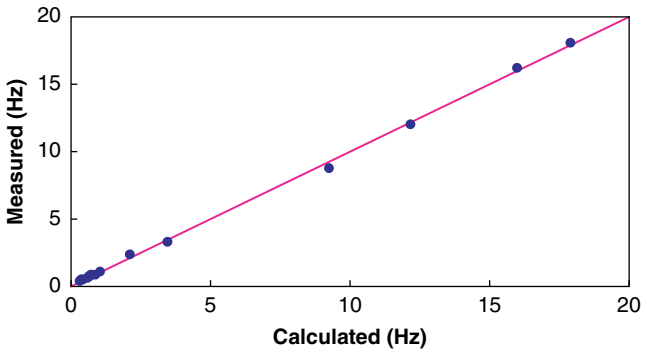

FIGURE 3 Comparison of calculated and measured frequencies.

correlation of the three calculated and identified mode shapes systematically, the modal assurance criterion (MAC) index (*13*) was computed for each mode as follows:

$$\mathrm{MAC}_{jk} = \frac{\left(\{\phi_j\}^T\{\hat{\phi}_k\}\right)^2}{\left(\{\phi_j\}^T\{\phi_j\}\right)\left(\{\hat{\phi}_k\}^T\{\hat{\phi}_k\}\right)} \tag{1}$$

where $\{\phi_j\}$ is the jth mode shape from the FEM and $\{\hat{\phi}_k\}$ is the kth mode shape identified from the measured accelerations. In this study, the mode shapes were extracted from the seismic records during the earthquake. Because of an insufficient number of accelerometers installed on the approach span, only the cable-stayed main span of

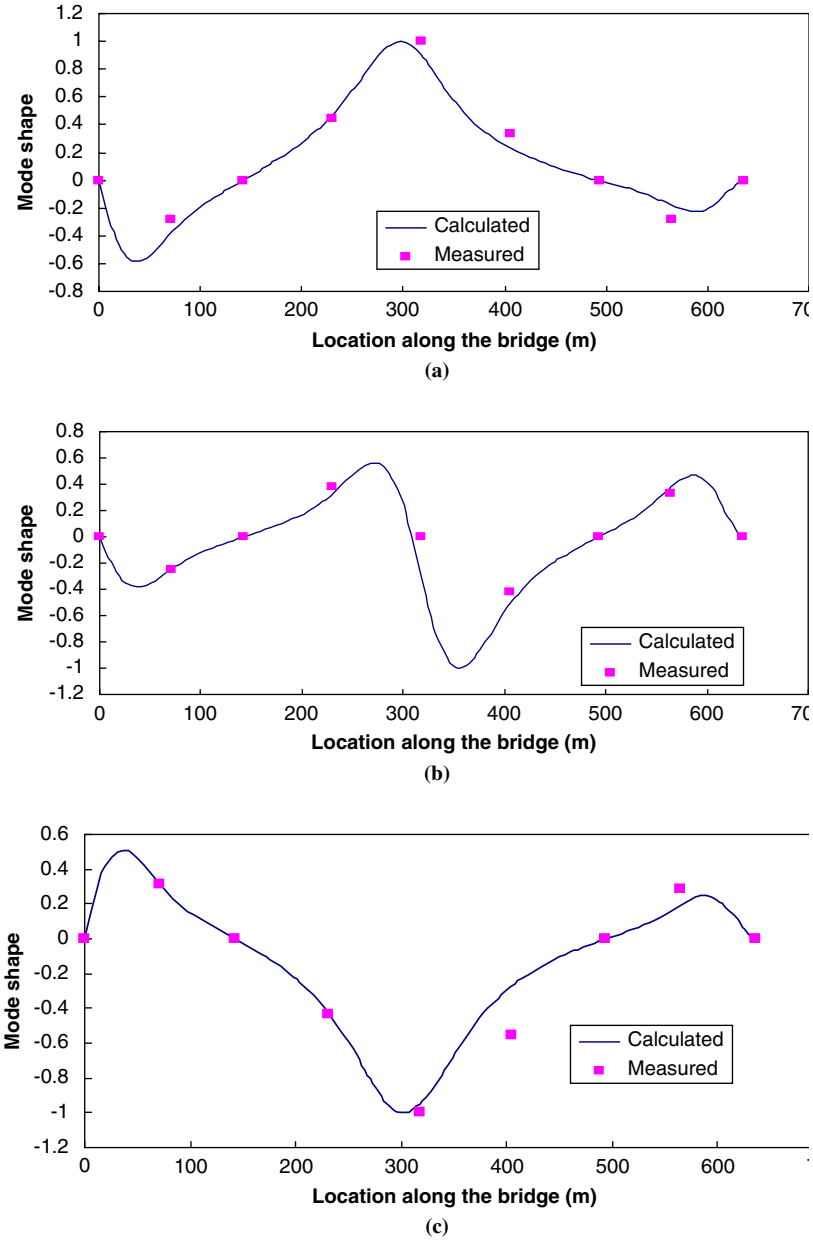

FIGURE 4 Comparison of calculated and measured mode shapes: (*a*) calculated versus measured first mode shape, (*b*) calculated versus measured second mode shape, and (*c*) calculated versus measured third mode shape.

the bridge was considered. In addition, the locations of accelerometers were estimated. The MAC values of the first, second, and third modes are 0.976, 0.837, and 0.950, respectively. Therefore, the calculated mode shapes correlate well with the identified mode shapes, particularly for the first and third modes of vibration.

SEISMIC PERFORMANCE EVALUATION OF BRIDGE

The rock motions recorded at the cable-stayed bridge generally reflect the regional geologic condition and tectonic characteristics around the NMSZ. Therefore, the bridge can be best assessed under a design earthquake that is scaled up from the rock motion recorded at the bottom of Pier 2 (Station D1) during the May 1, 2005, earthquake in Arkansas. The three acceleration components from Station D1 and their Fourier spectra are shown in Figure 5. On the basis of their Fourier spectra, the rock motions have a wide frequency range with a dominant frequency of approximately 10 Hz. To reach the peak acceleration corresponding to an M7.5 design earthquake (*14*), the recorded rock accelerations must be multiplied 10,000 times. The amplified peak acceleration reached 0.57*g* in the transverse and longitudinal directions and 0.42*g* in the vertical direction. The amplified three-component acceleration time histories are hereafter referred to as the design earthquake.

Because of their critical role in maintaining the structural integrity of the bridge, two towers and two typical cables were evaluated in detail. Under earthquake loads, the maximum moment likely occurs either at the bottoms of the two towers, B and D, or immediately above the capbeams, A and C on the tower columns, as illustrated in Figure 1. To determine the bending capacity of each section of the towers, moment curvature analysis was performed to evaluate the load–deformation behavior of a reinforced concrete section, with the Whitney stress block for concrete along with elastoplastic reinforcing steel behavior (*15*). The dimension and reinforcement distribution about sections were taken from the as-built bridge drawings.

After the bending moment demands were determined from the FEM of the bridge, the ratio of capacity over demand of each column can be evaluated. The maximum bending moment, the moment capacity, and the ratios of moment capacity over demand at the four critical locations—A, B, C, and D—are given in Table 2, in which M_x and M_y are the out-of-plane and in-plane bending moments of the towers under the design earthquake, and M_{xu} and M_{yu} are their corresponding capacities. The infill wall at each tower was not taken into account in the calculation of the moment capacity of each tower leg, which is a conservative assumption. It is clearly seen from Table 2 that the out-of-plane ratios of moment capacity over demand are all above 5.0, indicating an elastic behavior of the bridge or a conservative design for earthquake loads. In the plane of the tower frame, the bottom section of the tower has the ratio of moment capacity over demand of more than 1.73. If the infill wall at the lower portion of the towers were considered in the capacity calculation, the ratio of moment capacity over demand would increase. As such, the in-plane behavior of the bridge is also elastic at the bottom of the towers. Above the capbeam of the towers, however, the ratio of moment capacity over demand is approximately equal to 1.0, indicating that the towers experienced nearly inelastic behavior during the design earthquake, which agrees well with the original design criteria.

The maximum force and stress of all stay cables induced by dead plus earthquake loads were calculated. The ratio between the design stress and the maximum calculated stress (or design stress ratio) and the ratio between the material strength and the maximum calculated stress (or factor of safety) are shown in Figure 6 for all cable stays. It is evident that most design stresses are close to the maximum tensile stresses during a design earthquake. According to the as-built bridge drawings, the cables were made of ASTM A416, Grade 270, weldless, low-relaxation strands that have a yield strength of σ_y = 1,860 MPa. As indicated in Figure 6, all stay cables are in the elastic range under the dead plus earthquake loads. Figure 6 shows that the minimum factor of safety of 2.78 occurs in Cables 13 and 14 as illustrated in Figure 1, and the maximum factor of safety of 9.03 in Cable 17. This analysis ensures the safety of the cable-stayed bridge during a design earthquake.

The stress time histories in Cables 14 and 17 are given in Figure 7. The initial stress at the beginning of the earthquake represents the dead load effect, approximately 550 MPa. This finding means that the earthquake effect is approximately 669 − 551 = 118 MPa, which accounts for 22% of the dead load stress. As indicated in Figure 7, the minimum stress during the design earthquake is approximately 102 MPa, indicating that Cable 17 is always in tension and did not experience any slack. This analysis ensures that no cable was subjected to compression during the earthquake and thus all the analyses, by assuming linear cable elements for dynamic analysis, are acceptable.

Lateral earthquake restrainers and shock transmission devices significantly affect the dynamic responses of the bridge system. They can greatly reduce the maximum moment at the bottom of piers as shown in Table 3. The malfunction of the earthquake protective system may lead to a very flexible structure system. For example, the first natural frequency of transverse motions will significantly change from 0.53 Hz to 0.17 Hz. However, the first natural frequency of vertical motions will only decrease from 0.32 to 0.308 Hz with a reduction of approximately 4%. The first natural frequency of torsional motion will decrease from 0.53 Hz to 0.51 Hz with a reduction of approximately 5%.

The maximum axial force in all shock transmission devices under the design earthquake is 2.79 MN (626.7 kips), which is within their load capacity of 6.67 MN (1,500 kips). Each lateral earthquake restrainer is subjected to a maximum shear force of 3.5 MN (787 kips) under the design earthquake, which accounts for 11% of its load capacity, 30.8 MN (6,925 kips). Therefore, both shock transmission device and lateral earthquake restrainer are adequate in strength and expected to perform as designed.

CONCLUSIONS

A comprehensive three-dimensional (3-D) FEM of the Bill Emerson Memorial cable-stayed bridge was developed and validated with the earthquake ground motions and structural responses recorded during the M4.1 earthquake that occurred on May 1, 2005, in Arkansas. On the basis of extensive analyses of the bridge model, the following main conclusions can be drawn:

1. Rigid link elements were introduced in the FEM to connect cables properly to their supporting components. The geometric nonlinearity due to cable sagging must be taken into account in the modeling of a cable-stayed bridge. The diaphragm stiffness of the bridge decks can contribute to the natural frequencies by 7%~15%.
2. The computed natural frequencies of the 3-D FEM agree well with those from the field-measured data. The maximum frequency error of the first 16 significant modes is less than 10%. The mode assurance criterion index between a computed mode shape and its

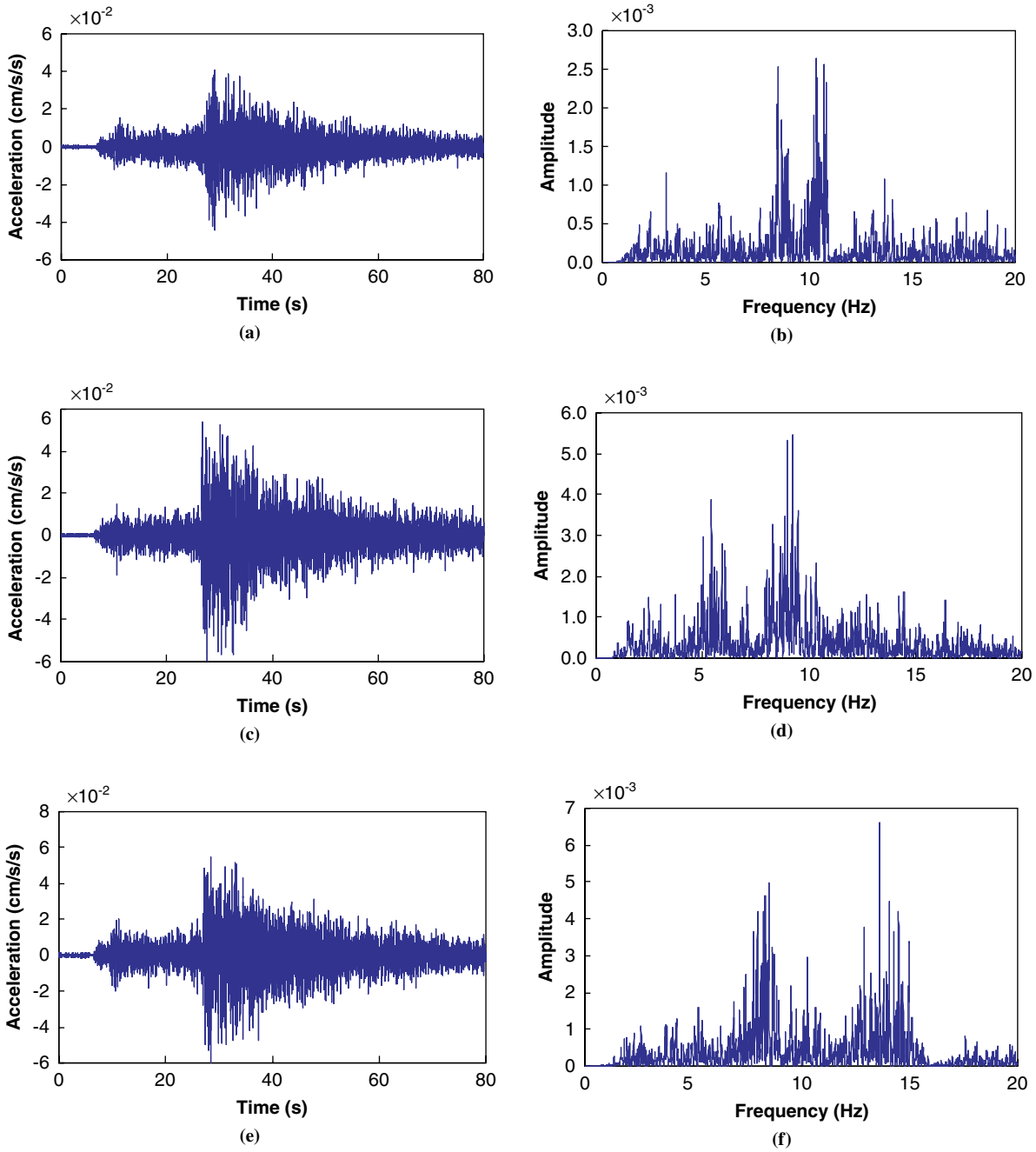

FIGURE 5 Rock motions at Station D1, Arkansas, 2005: (*a*) vertical acceleration time history, (*b*) vertical acceleration fast Fourier transform (FFT), (*c*) transverse acceleration time history, (*d*) transverse acceleration FFT, (*e*) longitudinal acceleration time history, and (*f*) longitudinal acceleration FFT.

TABLE 2 Ratios of Moment Capacity over Demand

Moment	Location			
	A	B	C	D
M_x(kN-m)	6.50×10^4	9.66×10^4	6.68×10^4	2.53×10^4
M_{xu}(kN-m)	4.14×10^5	4.87×10^5	4.14×10^5	4.87×10^5
M_{xu}/M_x	6.37	5.04	6.20	19.23
M_y(kN-m)	2.16×10^5	5.86×10^4	2.39×10^5	1.67×10^5
M_{yu}(kN-m)	2.43×10^5	2.89×10^5	2.43×10^5	2.89×10^5
M_{yu}/M_y	1.13	4.93	1.02	1.73

corresponding measured one is above 0.837 for the first three modes, indicating the general accuracy of the 3-D FEM in engineering applications.

3. All cables remain in tension and behave elastically under a postulated design earthquake with a factor of safety greater than 2.78. The two H-shaped towers always remain in the elastic range with a wide margin of safety except that the in-plane behavior of the hollow cross sections above the capbeams of the towers is near yielding under the design earthquake.

4. Longitudinal shock transmission devices and lateral earthquake restrainers significantly affect the overall behavior of the bridge system. Installation of these devices can greatly reduce the motion in the deck and also lower the stress level of the pier at the bottom. Under the design earthquake, both components were adequate and expected to function as designed.

ACKNOWLEDGMENTS

Financial support to complete this study was provided in part by the Missouri Department of Transportation and the U.S. Department of Transportation under the auspices of Center for Transportation Infrastructure and Safety, a national University Transportation Center at Missouri University of Science and Technology. Special thanks go to M. Celebi from the U.S. Geological Survey for assistance in retrieving the earthquake records from the May 1, 2005, earthquake.

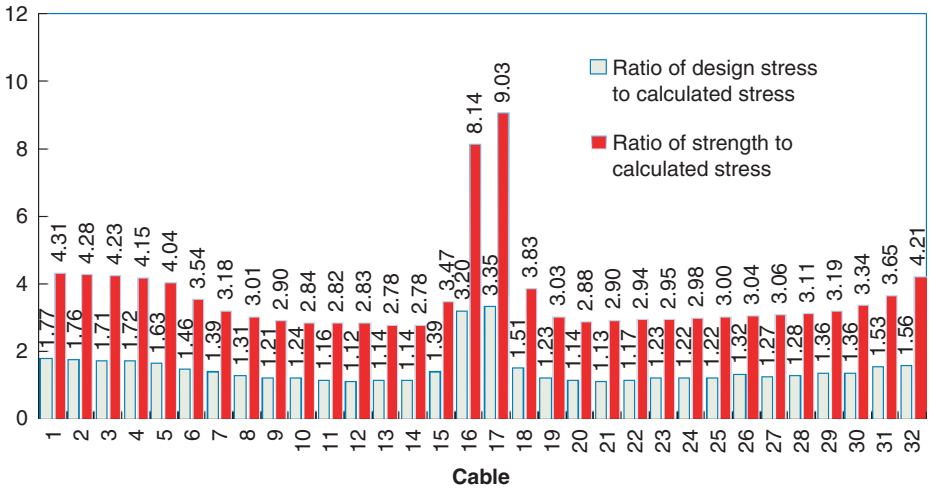

FIGURE 6 Safety coefficients of cables.

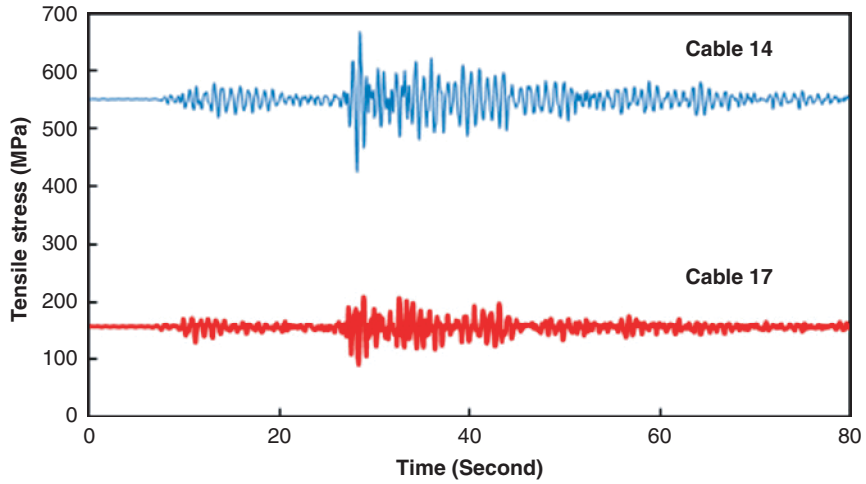

FIGURE 7 Time history of tensile stress in cables.

TABLE 3 Effects of Seismic Protective System

	FEM With SPS			FEM Without SPS		
Peak Response	L	T	V	L	T	V
Deck-to-tower displacement at Pier 2 (mm)	0	1.5	0	38.6	32.8	31.2
Deck acceleration at Pier 2 (mm/s^2)	657	4,970	4,580	5,320	5,710	3,360
Deck velocity at Pier 2 (mm/s)	118	204	72	147	270	12
Deck displacement at Pier 2 (mm)	86.6	60.9	33.3	86.1	32.0	34.1
Moment at base of Pier 2 (10^4 kN-m)	9.66	5.86	1.73	14.0	18.5	3.33
Moment at base of Pier 3 (10^4 kN-m)	2.53	16.7	2.73	12.0	27.6	4.49

NOTE: SPS = seismic protective system, L = longitudinal, T = transverse, V = vertical.

REFERENCES

1. Allam, S. M., and T. K. Datta. Seismic Behavior of Cable-Stayed Bridges Under Multi-Component Random Ground Motion. *Engineering Structures,* Vol. 21, 1999, pp. 62–74.
2. *Seismic Retrofitting Manual for Highway Bridges.* Publication FHWA-RD-94-052. FHWA, U.S. Department of Transportation, 1995.
3. Macdonald, J. H. G., and W. E. Daniell. Variation of Modal Parameters of a Cable-Stayed Bridge Identified from Ambient Vibration Measurements and FE Modeling. *Engineering Structures,* Vol. 27, 2005, pp. 1916–1930.
4. Ren, W. Ultimate Behavior of Long-Span Cable-Stayed Bridges. *Journal of Bridge Engineering,* Vol. 4, No. 1, 1999, pp. 30–37.
5. Ren, W., and M. Obata. Elastic-Plastic Seismic Behavior of Long Span Cable-Stayed Bridges. *Journal of Bridge Engineering,* Vol. 4, No. 3, 1999, pp. 194–203.
6. Nazmy, A. S., and A. M. Abdel-Ghaffar. Three-Dimensional Nonlinear Static Analysis of Cable-Stayed Bridges. *Computers and Structures,* Vol. 34, No. 2, 1990, pp. 257–271.
7. Abdel-Ghaffar, A. M., and A. S. Nazmy. 3-D Nonlinear Seismic Behavior of Cable-Stayed Bridges. *Journal of Structural Engineering,* ASCE, Vol. 117, No. 11, 1991, pp. 3456–3476.
8. Chen, G. D., N. Anderson, R. Luna, R. W. Stephenson, M. El-Engebawy, P. F. Silva, and R. Zoughi. *Earthquake Hazards Assessment and Mitigation: A Pilot Study in the New Madrid Seismic Zone.* CIES Technical Report 07-073. Center for Infrastructure Engineering Studies, University of Missouri, Rolla, 2005.
9. *AASHTO Standard Specifications for Highway Bridges,* 16th ed. American Association of State Highway and Transportation Officials, Washington, D.C., 1996.
10. Celebi, M. Real-Time Seismic Monitoring of the New Cape Girardeau Bridge and Preliminary Analysis of Recorded Data: An Overview. *Earthquake Spectra,* Vol. 22, No. 3, 2006, pp. 609–630.
11. Dyke, S. J., J. M. Caicedo, G. Turan, L. A. Bergman, and S. Hague. Phase I Benchmark Control Problem for Seismic Response of Cable-Stayed Bridges. *Journal of Structural Engineering,* ASCE, Vol. 129, No. 7, 2003, pp. 857–872.
12. Caicedo, J. M., G. Turan, and S. J. Dyke. Comparison of Modeling Techniques for Dynamic Analysis of a Cable-Stayed Bridge. *Proc., ASCE Engineering Mechanics Conference,* Austin, Tex., 2000.
13. Friswell, M. I., and J. E. Mottershead. *Finite Element Model Updating in Structural Dynamics.* Kluwer Academic Publishers, Dordrecht, Netherlands, 1995.
14. *Geotechnical Seismic Evaluation Proposed New Mississippi River Bridge (A-5076) Cape Girardeau, MO.* Woodward-Clyde Consultants, Totowa, N.J., 1994.
15. Wang, W. *Structural Condition Assessment of the Bill Emerson Memorial Cable-Stayed Bridge Using Neural Networks.* PhD dissertation. University of Missouri, Rolla, 2007.

The results and opinions are those of the authors only and do not necessarily reflect those of the sponsors.

The Seismic Design and Performance of Bridges Committee peer-reviewed this paper.